

A Compact Plasma Beam Dump for Next Generation Particle Accelerators

Lewis Boulton

9438793

School of Physics and Astronomy

University of Manchester

MPhys Project Semester 2 report

May 2018

This project was performed in collaboration with *Thomas Bullingham*.

Abstract

A new generation of compact particle accelerators, for example those based on Laser Wakefield Acceleration (LWFA), are in need of equally compact beam dumps in order to achieve the vision of low-cost and even mobile accelerator facilities. Plasmas are capable of supporting extremely strong decelerating gradients when excited by a strong particle beam and so form the basis for a new kind of compact beam dump that is studied in this report. In this project, a 1 GeV electron bunch modelled on the parameters provided by the EuPRAXIA project was used as a typical example of a beam produced by LWFA. Using the PIC code EPOCH, the effect of sending such a beam through uniform plasmas of different densities was simulated, followed by tests using a variety of different plasma structures in order to maximise the overall energy loss of the beam. Results show that initial decelerating gradients of 75 GV/m are achievable and are able to reduce the energy of the beam to 40% of its initial value after a distance of around 1.5 cm. Furthermore, by using a linearly increasing plasma density to remove any reaccelerated electrons from the beam, further reduction to around 10% of the initial energy was achieved over a distance of less than 10 cm in total.

1 Introduction

Particle accelerators are now ubiquitous in many areas of scientific research, for example in high energy particle collider experiments and sources of synchrotron radiation. However, once they have served their purpose, the high energy beams need to be disposed of safely. Most facilities rely on dense materials such as water, metal or graphite to absorb the beam's energy. This method primarily involves the loss of energy via coulomb collisions with the stopping materials atoms, inevitably leading to the degradation of the beam dump material and the production of radionuclides which can be harmful to humans if not dealt with appropriately [1]. Another pressing issue is the physical size of these conventional beam dumps, which need to be very long in order to fully absorb the beam's energy. For instance, a proposed gas based beam dump for the International Linear Collider (ILC) would need to be around 1000 m in length [2]. This can further increase the cost of already large, expensive facilities, but would also defeat the purpose of the next generation of high energy compact accelerators (such as laser driven plasma accelerators) if whole buildings are necessary to house their beam dumps.

Interestingly however, similar physics to that involved in plasma wakefield acceleration has been suggested as the basis for a new kind of particle beam dump. By using a driving laser or particle beam propagating through a plasma channel, plasma accelerators are able to generate extremely high electric fields in the regions of charge separation that follow in the wake of the drive beam [3]. These so called wakefields can then be used to accelerate charged particles to high energies over very short distances. As well as regions of high accelerating gradients, plasma accelerators also support areas with large decelerating gradients. Whereas these decelerating regions can prove problematic in plasma wakefield acceleration schemes, some believe they can be exploited for the purposes of a new compact particle beam dump, as shown in Figure 1.

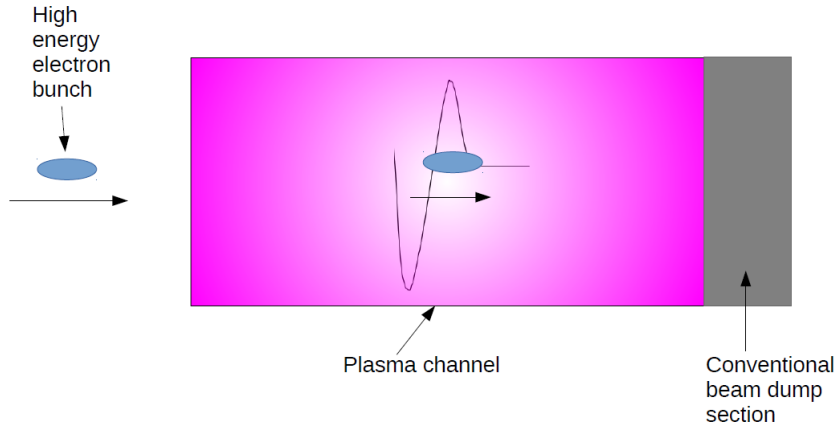


Figure 1: A schematic drawing of a plasma beam dump. The high energy electrons enter the plasma channel and experience large decelerating gradients. Any residual energy can then be absorbed by conventional material, for example. The overall beam dump would then be much more compact than one made from purely conventional materials.

By using the PIC (Particle In Cell) code EPOCH [4] to simulate an electron beam propagating through a plasma, this project aims to demonstrate the feasibility of such a plasma beam dump as a stopping medium for the ultra short, high energy bunches that are routinely produced by plasma based accelerators. In particular we use beam parameters predicted to be achieved by

EuPRAXIA, an international project that aims to design and eventually build a cost-effective plasma accelerator facility in Europe [5]. These parameters are summarised in Table 1.

Parameter	Value
Mean beam energy, T_0	1-5 GeV
RMS energy spread	$\sim 5\%$
RMS bunch length, σ_z	$1.5 \mu\text{m}$ (5 fs)
RMS transverse beam size, $\sigma_{x,y}$	$\sim 0.3 \mu\text{m}$
Bunch charge	100 pC
Peak bunch density, n_b	10^{23} m^{-3}

Table 1: Potential beam parameters for beams produced by plasma accelerators in the EuPRAXIA project.

2 Theory

2.1 Stopping Power in Condensed Matter

Any discussion of the interaction of electrons with matter as they travel through a material will inevitably begin with the classic Bethe-Bloch formula [6] [7],

$$-(\frac{dT}{dx})_I = (\frac{F}{\beta^2})[\ln(2m_e\gamma^2v^2/I) - \beta^2], \quad (1)$$

where T is the electron's kinetic energy, I is the specific average ionisation energy of the stopping medium, $\beta = \frac{v}{c}$ is the particle's normalised velocity and γ is its' relativistic factor. Furthermore, $F = e^2k_{pe,m}^2n_{e,m}$, where e is the charge of the electron, $k_{pe,m}$ is the plasma wavenumber of the stopping medium and $n_{e,m}$ is the number density of the material. In this treatment of stopping power, the dominant contribution to energy loss of the electrons comes from the ionisation of the atoms in the stopping material.

However, for higher energy electrons (namely those with $T > 100$ MeV), an important and in fact dominating contribution to the energy loss of electrons traversing a material is due to brehmsstrahlung radiation emitted during collisions with the stopping mediums atoms. The stopping power from this contribution is given by the formula [8]

$$-(\frac{dT}{dx})_R = F(\frac{Z}{137\pi})(\gamma - 1) \ln(183Z^{-\frac{1}{3}}), \quad (2)$$

where Z is the atomic number of the beam dump material. As the energies of the electron beams in this project are of order 1 GeV, Equation (2) best describes the energy loss due to binary interactions between the electrons and the stopping atoms.

2.2 Stopping Power in Plasmas and Collective Deceleration

As demonstrated by Ichimaru [9], the Bethe-Bloch formula for the stopping power in a plasma can be split into two contributions, such that

$$-(\frac{dT}{dx})_{plasma} = -(\frac{dT}{dx})_{bin} - (\frac{dT}{dx})_{coll}. \quad (3)$$

The first term as before is due to the binary interactions between the beam electrons and the plasma particles, which in the high energy regime is described by Equation (2). The second term on the other hand can be attributed to the long-range collective interaction between the electron beam and the plasma, given by

$$-(\frac{dT}{dx})_{coll} = (\frac{F}{\beta^2}) \ln(\frac{k_D v}{\omega_p}), \quad (4)$$

where k_D is the Debye wavenumber and ω_p is the plasma frequency, a key quantity in plasma physics, given by [10]

$$\omega_p = \sqrt{\frac{n_p e^2}{m_e \epsilon_0}}. \quad (5)$$

Here, n_p is the number density of the plasma electrons, whilst ϵ_0 is the permittivity of free space. The contribution given by Equation (4) corresponds to the interaction between the collectively excited plasma oscillations and the incoming electron bunches, which at long ranges can be considered as single point particles.

Equation (4) however is only valid in the linear regime, where perturbation theory can be applied to find the collective effects due to the excited plasma. When excited by a strong laser pulse or high-current relativistic particle beam, the collective interaction due to the plasma becomes highly non-linear and therefore impossible to solve analytically. It can however be characterised by the limit of the so called 'wave-breaking' field, as illustrated by G.Mourou et al [11], where

$$E_{WB} = \frac{m_e c \omega_p}{e}. \quad (6)$$

W.Lu et al. [12] gives a further modification to this formula for the case of a wakefield generated by an electron beam, such that the limit of the wave-breaking field is proportional to the ratio $\frac{n_b}{n_p}$, where n_b is the number density of the electron beam. The stopping power in this limit is therefore given by

$$-\left(\frac{dT}{dx}\right)_{WB} = m_e c \omega_p \left(\frac{n_b}{n_p}\right). \quad (7)$$

Equation (7) suggests that in order to provide optimal deceleration a dense electron beam is required, $n_b > n_p$. However, if the field generated is too strong, plasma electrons may be self-injected into the accelerating part of the wakefield. To compromise it is therefore sensible to use $n_b \sim n_p$. Note that the electron beams in this project are assumed to be spatially gaussian, such that their peak number density is given by

$$n_b = \frac{N_b}{(2\pi)^{\frac{3}{2}} \sigma_x \sigma_y \sigma_z}, \quad (8)$$

where N_b is the total number of electrons in the bunch and σ_z and $\sigma_{x,y}$ are the bunch dimensions in the longitudinal and transverse directions respectively. For $n_p \sim n_b \sim 10^{18} \text{ cm}^{-3}$, Equation (7) gives a decelerating gradient of approximately 96 GeVm^{-1} , whereas for a conventional copper beam dump, Equation (2) gives an initial stopping power of around 5 GeVm^{-1} , meaning plasma beam dumps in theory only need to be around a tenth of the size of their conventional counterparts.

2.3 Saturation and Plasma Beam Dump Schemes

Although their stopping power can be potentially much greater than that provided by conventional beam dumps, plasma beam dumps have a number of issues. One main issue is that of re-acceleration. As the electrons in the decelerating beam lose enough energy such that they become sub-relativistic, they begin to slip backwards in to the accelerating region of the wakefield. As this happens, the electrons can become caught and re-accelerated, meaning that the mean energy loss of the beam decreases. At this point the energy loss has become saturated, and the distance through a uniform plasma at which this occurs is known as the saturation length which can be approximated as

$$L_{sat} \approx \frac{T_0}{eE_{dec}}, \quad (9)$$

where T_0 is the initial electron kinetic energy, e is the charge of the electron and E_{dec} is the peak decelerating field acting on the electron bunch. For a 1 GeV beam experiencing a wakefield with decelerating gradient of order 100 GV/m (as estimated by Equation 7), Equation 9 predicts that saturation will occur over distances of order 1 cm. To address this issue, the approach is to remove the low-energy electrons from the beam before they can be reaccelerated.

Two schemes are suggested by H.C.Wu et al. [8]. One involves introducing periodic vacuum gaps within the uniform plasma beyond the saturation length. The low-energy electrons become trapped within the evacuated regions and are consequently removed from the beam before they

are reaccelerated. A modification of this scheme is to use a sinusoidally varying plasma density, such that the changes in plasma density are less sudden, leading to less instability in the generated wakefields- both of these structures are sketched in Figure 2. Also suggested is the introduction of thin foils into the plasma (see Figure 3) in which low energy electrons will then become trapped. A key variable for these schemes will be the period of these structures, with the obvious characteristic length of choice being the plasma wavelength, $\lambda_p = \frac{2\pi c}{\omega_p}$.

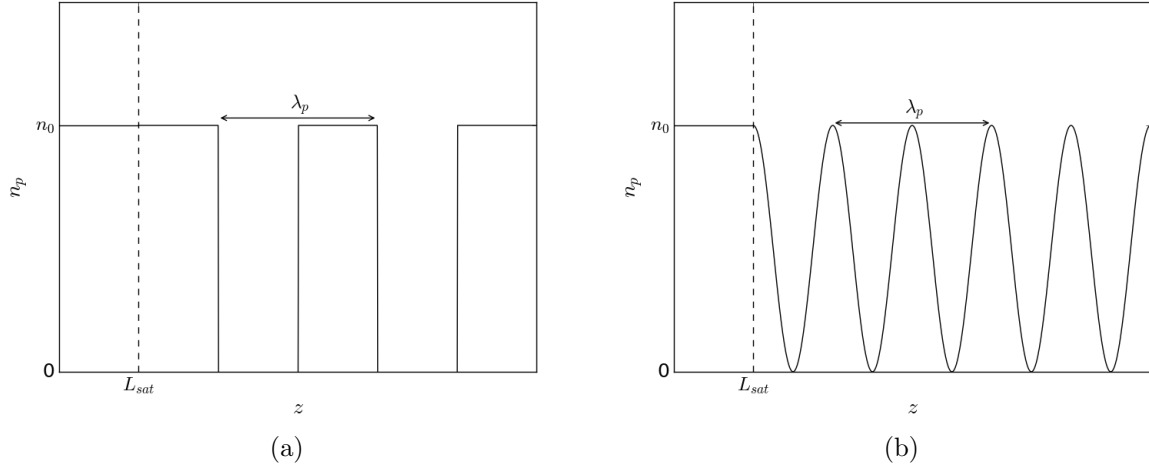


Figure 2: Sketches of the plasma density n_p vs the longitudinal coordinate z in the (a) vacuum gap and (b) sinusoidal profile schemes. Up until the saturation length L_{sat} the plasma density remains uniform at n_0 . The sinusoidal function is essentially a squared cosine function of period λ_p . In both cases the period could be changed to other multiples of λ_p , but shall remain at a constant value for this project.

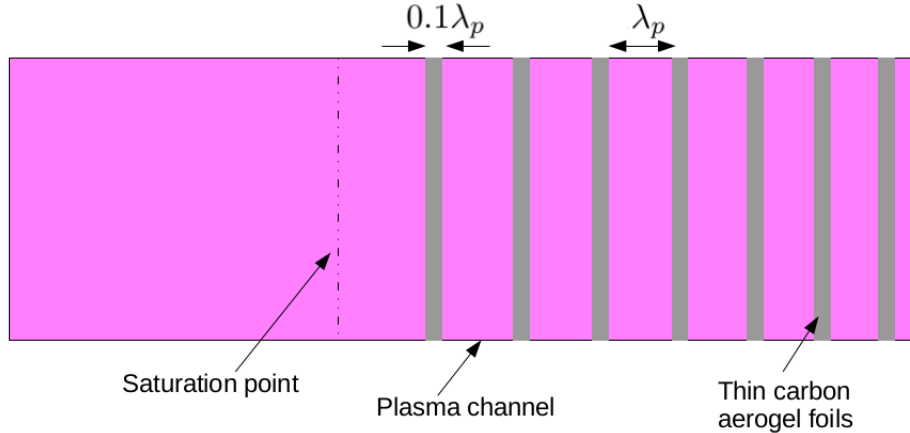


Figure 3: A schematic drawing of how thin carbon aerogel foils can be inserted into the plasma beyond the saturation length. As shown, the spacing of these foils is λ_p in this project, but could be changed to other multiples of λ_p in other studies. The thickness of the foils themselves on the other hand is $0.1\lambda_p$.

Rather than trapping the low energy electrons, another method is to remove the electrons via defocusing. This is achieved by increasing the density of the plasma as the beam travels beyond the saturation length. This defocusing region is located approximately $\frac{\lambda_p}{4}$ behind the decelerating section, and removes low energy particles from the axis as they pass through. Hanahoe et. al [13] gives some proposed density functions including examples that increase linearly and quadratically with distance, as shown in Figure 4.

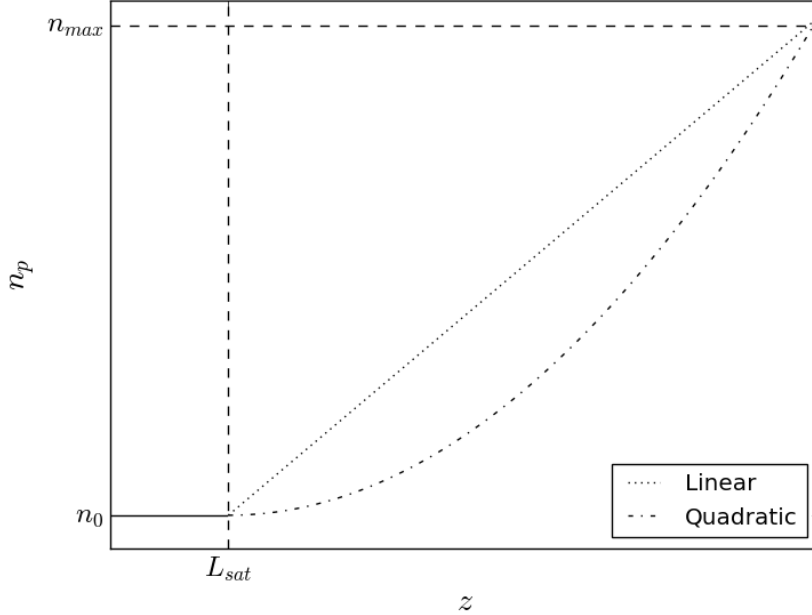


Figure 4: A sketch of the plasma density n_p vs the longitudinal coordinate z for linear and quadratic density profiles. Up until the saturation length L_{sat} , the plasma density remains uniform at n_0 . The two profiles then increase at a rate such that they both reach n_{max} after the same distance.

In these schemes it is key to consider the rate of increase of the plasma density. Although a steeper density results in the decelerated electrons regaining less energy, a denser plasma generates weaker decelerating wakefields. Furthermore, the plasma densities have to be low enough to be achievable in practice.

3 Experimental Approach

3.1 Introduction to EPOCH

EPOCH (Extendable PIC Open Collaboration) is an open-source plasma physics simulation code created as part of the Collaborative Computational Project In Plasma Physics. The code, like many others of its kind, utilizes the Particle In Cell method, where collections of physical particles are represented by small numbers of pseudoparticles, whose positions are mapped onto a fixed grid of cells. From the charge distribution formed by these particles, the fields generated within the simulation can be calculated using the Finite Difference Time Domain method, in

which the time-dependent Maxwell's equations are discretized and solved [14]. From this the velocities of the pseudo-particles inferred. Using these velocities, the positions of the particles on the underlying grid are updated and the process repeats.

Control of EPOCH is performed through the creation of input decks, in which the user specifies the different parameters of the simulation domain. These scripts are composed of several blocks, each controlling specific aspects of the simulation. For instance, the species block is where the type of particles used in the simulation is defined by specifying their charge and mass, as well as their initial density and momentum distributions. Other blocks include the control block, where the underlying grid is specified, and the boundaries block, where the behaviour of particles at the simulations edges are defined (e.g reflecting, outflow etc.) In this particular project, it is wise to use a moving window such that the electron beam remains in the same position in the simulation domain, where plasma is essentially introduced at one boundary and removed at the others.

Data from an EPOCH simulation is contained within Self-Describing Data Files (SDF), which are produced every time the simulation performs an output dump (as controlled by the output block in the input deck.) These files can only be read by compatible software- in this case, Python was used and the data visualised using the Matplotlib package [15]. Information outputted by EPOCH can be attributed to either individual particles (e.g a specific particles kinetic energy, position, velocity etc.) or the simulation grid itself (e.g electric field, number density etc.). An important quantity to consider in all analysis of the data produced by EPOCH is the weight attributed to each pseudoparticle i.e how many 'real' particles a certain pseudoparticle represents.

3.2 Simulations Outline

For the purposes of this project, the 2D version of EPOCH was sufficient, assuming that the system is symmetrical about the direction of propagation i.e only consider longitudinal motion and the motion in one of the transverse planes. Before any beam dump simulations could be performed, an electron beam was first generated using EPOCH without a plasma present. This was achieved by creating a species of electrons that had a Gaussian density profile in the longitudinal and transverse planes. Based on the electron bunches that are predicted to be produced by LWFA in the EuPRAXIA project, the parameters for the beam in this project were chosen, as shown in Table 2.

Once satisfied that the simulation was able to produce the desired electron bunch, an initially uniform plasma was introduced, consisting of argon ions surrounded by their delocalised plasma electrons. In order to save on computational power, the ions in these simulations were immobilised- an approximation often used in the theory of plasma oscillations, as the ions are much heavier than the plasma electrons. To visualise the wakefields being generated at each stage in the simulation, the number density of the perturbed plasma could be plotted, as well as the electric field in the longitudinal direction.

To study the energy loss of the beam as it travelled through the plasma, the total kinetic energy of the beam electrons was found as a fraction of the initial total beam energy for each output dump and plotted as a function of distance travelled in the longitudinal direction. This, as well as plots of the longitudinal phase space, give some indication of when the energy loss has saturated for the electron beam. Several simulations were performed using a uniform plasma of different

Parameter	EUpraxia Beam	Simulation Beam
Mean beam energy, T_0	1-5 GeV	1 GeV
RMS energy spread	$\sim 5\%$	$\lesssim 1\%$
RMS bunch length, σ_z	$\sim 1.5\mu\text{m}$ (5 fs)	$1.5\mu\text{m}$ (5 fs)
RMS transverse beam size, $\sigma_{x,y}$	$\sim 0.3\mu\text{m}$	$0.3\mu\text{m}$
Bunch charge	100 pC	100 pC
Peak bunch density, n_b	10^{23} m^{-3}	10^{23} m^{-3}

Table 2: A table comparing the EuPRAXIA beam parameters to those used in this project. Note that the energy spread in these simulations is a lot less than realistically achievable in the EuPRAXIA beams. This is due to the fact that a large temperature was needed to give the beam a reasonable energy spread, which in turn required more computational power than available.

densities each time, specifically where $\frac{n_p}{n_b} = 1, 2, 5, 10$ and 0.1 . The energy loss for each of these cases could then be compared on the same graph, and the best result (i.e the one which reaches saturation the quickest) used as the basis for further simulations.

Using EPOCH's ability to restart simulations from an existing SDF file, different plasma schemes were trialled for the section of plasma beyond the saturation length, as outlined in Section 2.3. Again, for each of these cases, the further energy loss of the beam could be plotted simultaneously in order to compare the effectiveness of each of these schemes in reducing/preventing the re-acceleration of low energy electrons.

4 Results

The following section summarises the results obtained in this project, first studying the energy loss from propagation through a uniform plasma. Using the best parameters from these results, the simulation was then continued beyond saturation, where the effects of different plasma structures could be studied.

4.1 Uniform Plasma

A beam with parameters given in Table 2 was first simulated passing through a region of plasma whose density profile was uniform. Using data outputted at regular points throughout the beams trajectory, key aspects of the simulation could be visualised.

Figure 5 shows the evolution of the electric field in the z direction as the beam travels through a uniform plasma. These plots show initially efficient generation of wakefields, with a maximum decelerating gradient of approximately 75 GV/m in Figure 5 (a). However, as the beam propagates and loses energy, the quality of the wakefields decrease such that the maximum decelerating gradient in Figure 5 (d) is around 15 GV/m. In each of these plots, the beam is located at around $Z=15\mu\text{m}$, such that the beam tail experiences the decelerating electric field.

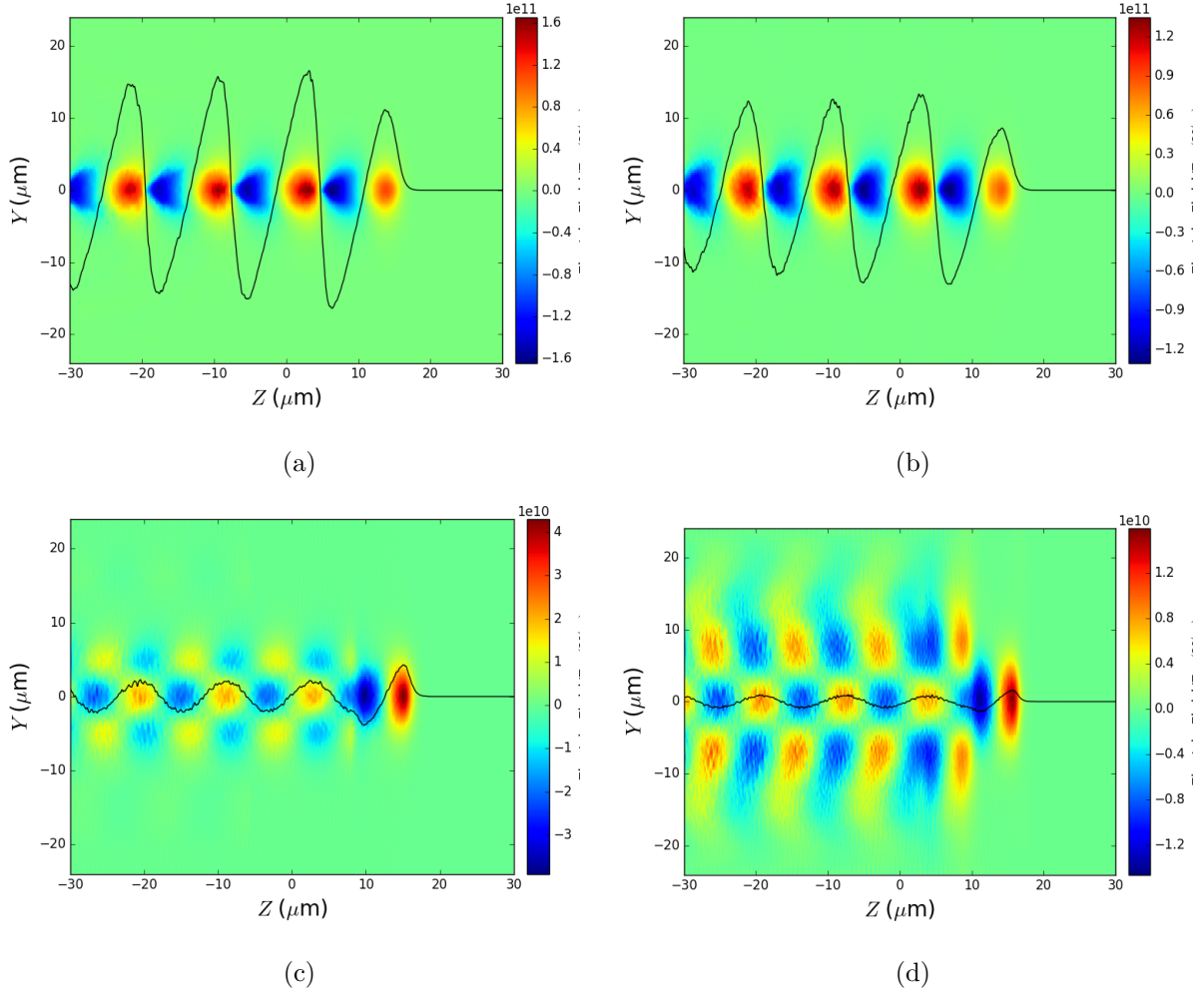


Figure 5: 2D colour mesh plots showing the electric field in the longitudinal direction, where the distance travelled by the electron bunch in each plot is (a) 0.1 cm, (b) 1 cm, (c) 2 cm and (d) 5 cm. Here Z and Y represent the longitudinal and transverse coordinates respectively in the reference frame of the moving simulation window. Here, the colorbars are in units of (V/m) and the solid black lines represent the relative electric field in the longitudinal direction along the line $Y = 0$. Note that these plots were taken from simulations where $\frac{n_p}{n_b} = 2$.

Figure 6 shows the effect of the generated wakefields on the longitudinal phase space of the electron beam. Figures 6 (a) and 6 (b) show the initially rapid deceleration of the bunch's tail particles such that some have reached sub-relativistic energies and are beginning to slip backwards towards the accelerating region of the wakefield. Figures 6 (c) and (d) then illustrate how these low energy electrons begin to regain energy, suggesting that the energy loss has saturated at these distances. A key feature of these plots is the fact that the energies of the electrons at the head of the beam show little change.

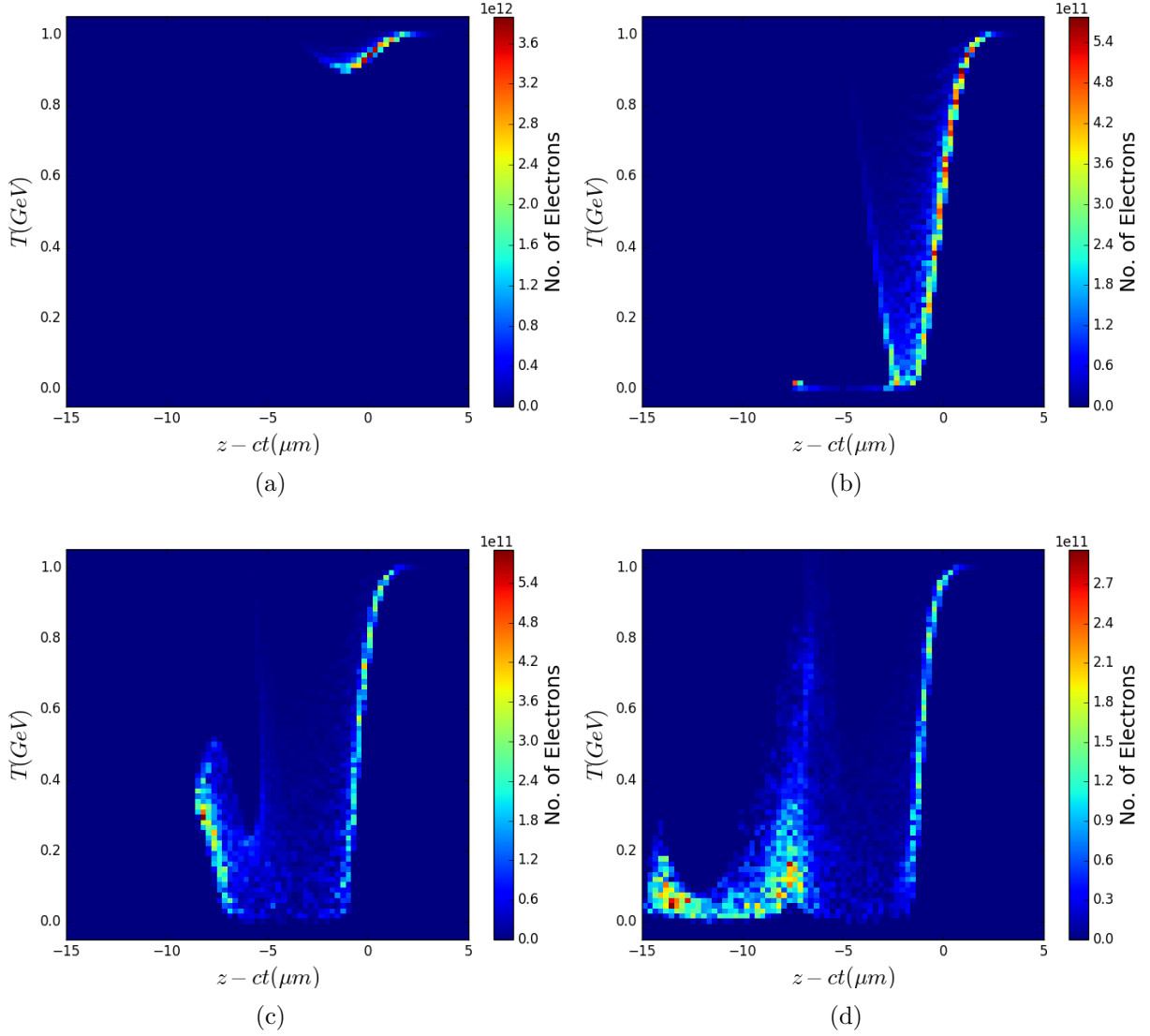


Figure 6: 2D density histograms of the electron bunch's longitudinal phase space, where the distance travelled by the electron bunch in each plot is (a) 0.1 cm, (b) 1 cm, (c) 2 cm and (d) 5 cm. Here the horizontal axis represents the longitudinal position with respect to the beam's initial centroid position within the simulation, whereas the vertical axis is T , the electron kinetic energy. Note that these plots were taken from simulations where $\frac{n_p}{n_b} = 2$.

So that the overall energy loss of the beam could be visualised, the total energy of the beam as a fraction of the initial total energy was plotted against the distance travelled by the beam. This was performed for different values of the uniform plasma density, with the results summarised in Figure 7. This plot shows that the most efficient energy loss is given by plasma densities of $\frac{n_p}{n_b} = 1$, 2 and 5, where the energy saturates at around 40% after a distance of approximately 1.5 cm. However, for the more extreme densities i.e. $\frac{n_p}{n_b} = 0.1$ and 10, the energy losses are much smaller, indicating that decelerating fields cannot be efficiently generated when the plasma is too tenuous or too dense. As the energy loss plateaus slightly sooner for the case where $\frac{n_p}{n_b} = 2$, this density was used for all further simulations.

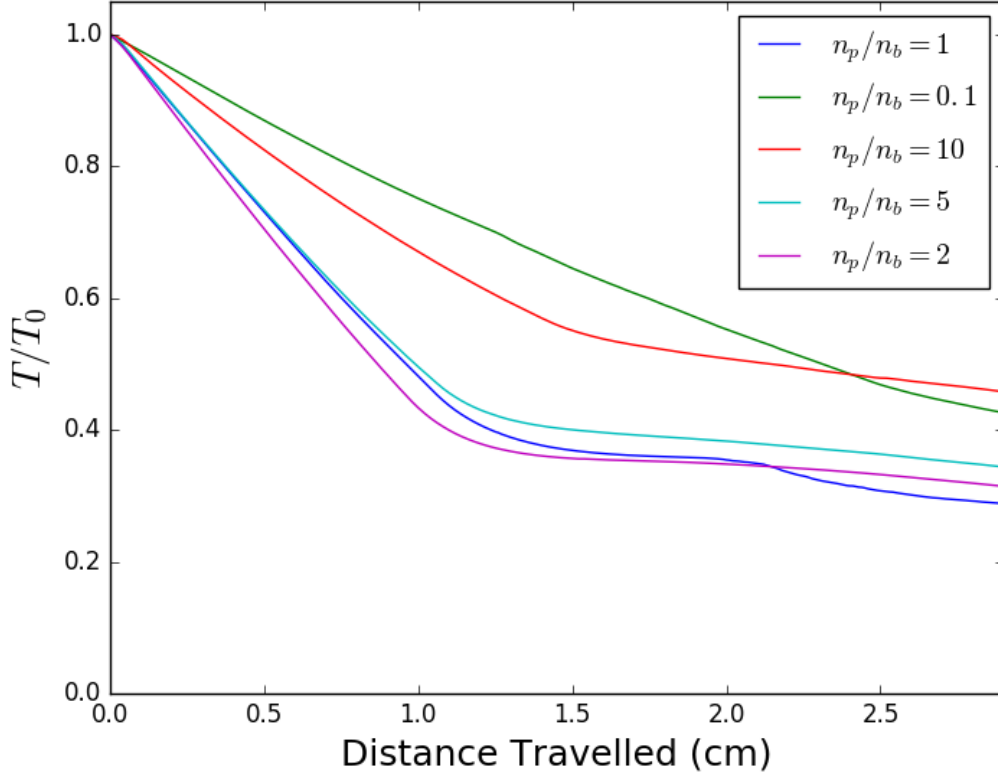


Figure 7: A plot of the total energy of the beam T as a fraction of the initial total energy of the beam T_0 vs the distance travelled by the electron beam. Each line represents a simulation with a different value of the plasma density with respect to the beam density $\frac{n_p}{n_b}$.

4.2 Structured Plasmas Beyond Saturation

In order to further decrease the energy of the electron beam beyond the saturation length, the reaccelerated particles needed to be removed using methods discussed in Section 3.2. Different density structures were introduced beyond a distance of 5 cm, such that a significant amount of electrons had begun to be reaccelerated.

Figure 8 shows the longitudinal phase space plots for the scheme that introduced vacuum gaps after the saturation length. By comparing the plot in Figure 6(d) with Figures 8(a) and 8(b), one sees a gradual decrease in the amount of electrons present in the bunch tail as the beam propagates, suggesting that some of the low energy particles are being trapped within the vacuum spaces. The scheme that involved a sinusoidally varying plasma and also the one that introduced periodic thin carbon aerogel foils into the plasma both involve similar mechanisms for removing low energy electrons from the beam and so their longitudinal phase spaces show similar evolution to that seen in Figure 8.

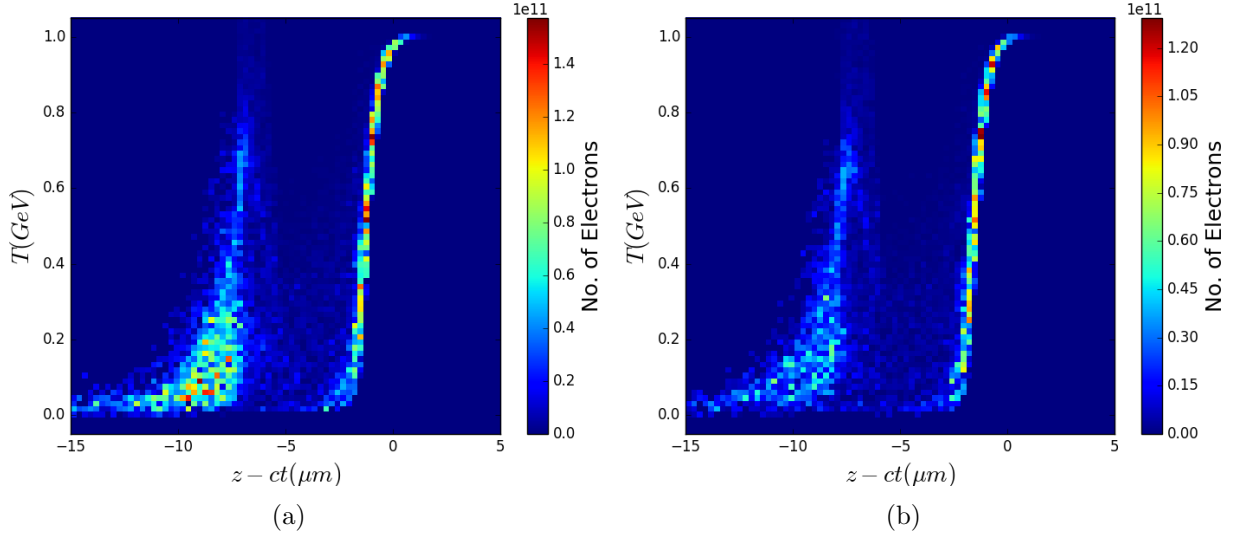


Figure 8: 2D density histograms of the electron bunch's longitudinal phase space in a plasma containing vacuum gaps, where the distance travelled in each plot is (a) 6 cm and (b) 8 cm.

Another mechanism for the removal of low energy electrons is the increase of the plasma density beyond the saturation length. Figure 9 shows the longitudinal phase space plots for a linearly increasing plasma density profile. Again, by comparing Figure 6(d) with Figures 9(a) and 9(b), the removal of low energy electrons at the tail of the bunch can be seen as the beam propagates, due to the defocussing effect described in Section 2.3.

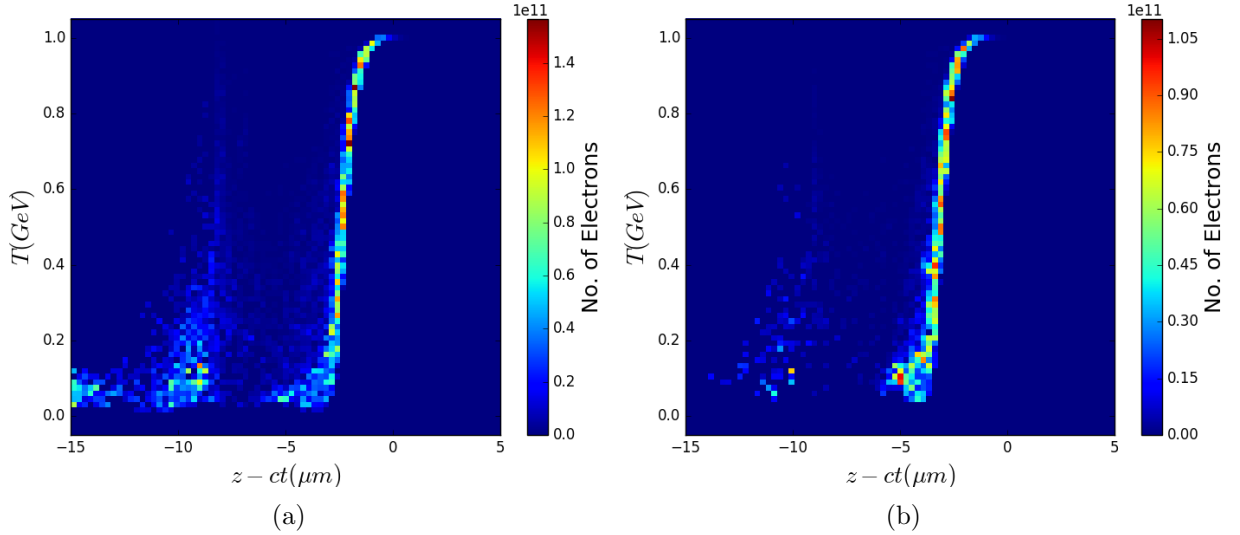


Figure 9: 2D density histograms of the electron bunch's longitudinal phase space in a plasma of linearly increasing density, where the distance travelled in each plot is (a) 6 cm and (b) 8 cm.

To compare the effects of using a different density structures beyond the saturation length, the energy loss was plotted simultaneously for each scheme, as shown in Figure 10.

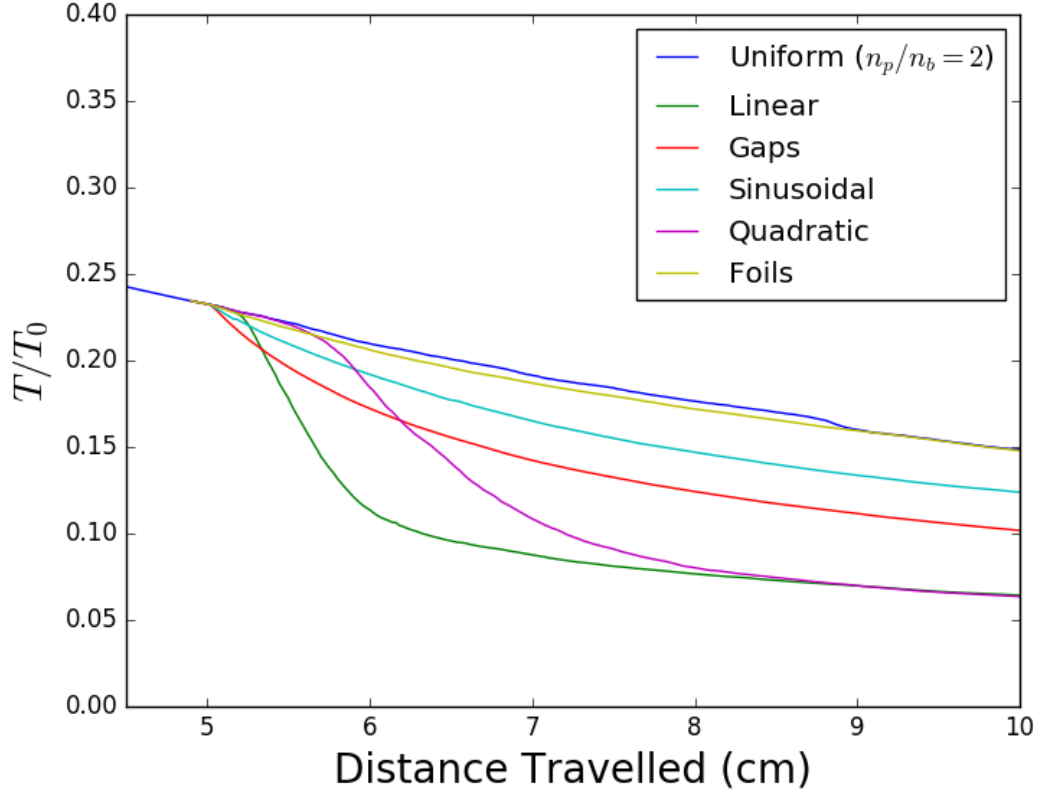


Figure 10: A plot of the total energy of the beam T as a fraction of the initial total energy of the beam T_0 vs the distance travelled by the electron beam. Each line represents a simulation using a different plasma density structure. These simulations were all restarted at a distance of 4.5 cm, but the changes to the density do not occur until after 5 cm.

Figure 10 shows that the energy of the electrons can again be decreased to under 10% of their initial value before the energy loss again becomes saturated. However, saturation in this case occurs once all of the re-accelerated electrons have been removed from the beam and only the head electrons remain. From Figure 10 it can be seen that the linearly increasing plasma density provides the most effective method of removing the re-accelerated electrons in order to further decrease the beam energy.

5 Discussion

Despite the apparent degradation of the generated wakefields shown in Figure 5 as the beam propagates, Figure 7 shows that for sensible plasma densities (i.e. $\frac{n_p}{n_b} \sim 1$), saturation can be reached after a distance of around 1.5 cm, which compares well with that predicted by Equation (9).

Due to saturation, around 40% or more of the beam energy remains, meaning further considerations are indeed necessary. By considering the energy loss curves in Figure 10, the linear density increase provides the most efficient energy loss beyond saturation of any of the density schemes by a large margin. Although the quadratic profile is also effective, the complete removal

of the re-accelerated electrons occurs later than in the linear case. However, this can easily be attributed to the fact that the rate at which the low energy electrons are removed is dependent on the gradient of the density increase. Whereas the gradient of the linear profile is at a constant value, the quadratic profile only begins to remove electrons when it's gradient becomes high enough.

The introduction of vacuum gaps beyond the saturation length and the analogous sinusoidal scheme exhibit similar behaviour with regards to Figure 10 i.e a gradual decrease in the beam energy as the re-accelerated electrons become trapped. Nevertheless, the vacuum gap method gives the best rate of energy loss of the two schemes. Further simulations may want to consider the effect that changing the period of the structure may have (i.e in multiples of λ_p).

However, the simulation involving the introduction of thin carbon aero gel foils periodically into the plasma performs far worse than would be anticipated for a real experiment. In this project, the foils were simulated as thin blocks of very dense, immobile plasma. In reality, there are a lot more effects to take in to account such as the collisions and ionisation of the foil atoms from the electron beam. Although not primarily designed to study particle interactions with solids, EPOCH does possess input deck blocks that deal with this kind of physics, and could perhaps be utilised in subsequent studies. This however would likely require more computing power than available in this project.

It should also be noted that in the uniform density case, the beam does still continue to lose energy, albeit at a much lower rate than before saturation has occurred. This is likely due to the natural loss of electrons from the beam to the plasma, and also the fact that the head electrons are still experiencing a small decelerating field.

An important consideration is the practicality of these density schemes in a real experiment. In practice, the plasmas with smoothly increasing density profiles may be more achievable than the sinusoidal and vacuum gap schemes, which require very organised structures to be formed at microscopic length scales. As well as being difficult to produce, any foil that is introduced to trap low energy electrons would also be subject to degradation in reality.

Although not critically important with regards to the wakefields generated in the plasma, it was mentioned in Section 3.2 that the energy spread of the simulation beam was much lower than reasonably achievable by the EUPRAXIA project. Regardless, in future studies the full energy spread should be taken into account such that the beam is as close to its' real counterpart as possible.

One main issue with the passive plasma beam dump is the fact that the electrons at the head of the beam experience very little deceleration, and by the time the re-accelerated electrons have been removed around 10% of the original beam energy is being carried by these remaining particles. An obvious solution is to have a small section of conventional material to absorb the residual energy. Such a beam dump would still be much shorter than a purely conventional beam dump, and would also produce a lot less radionuclides.

A slightly more elegant solution however is to excite wakefields within the plasma using a strong laser pulse, either before the beam dumping process has begun or at the point where only the head electrons remain, as shown in Figure 11. A. Bonatto et al. [16] gives the theory involved

in an active beam dump (i.e. wakefield excitation with a laser) and draws comparisons with passive beam dumps, like that studied in this project. Here it is argued that the net wakefield generated can potentially be stronger and more homogeneous than that in a passive dump (i.e. less degeneration of the decelerating fields as shown in Figure 5).

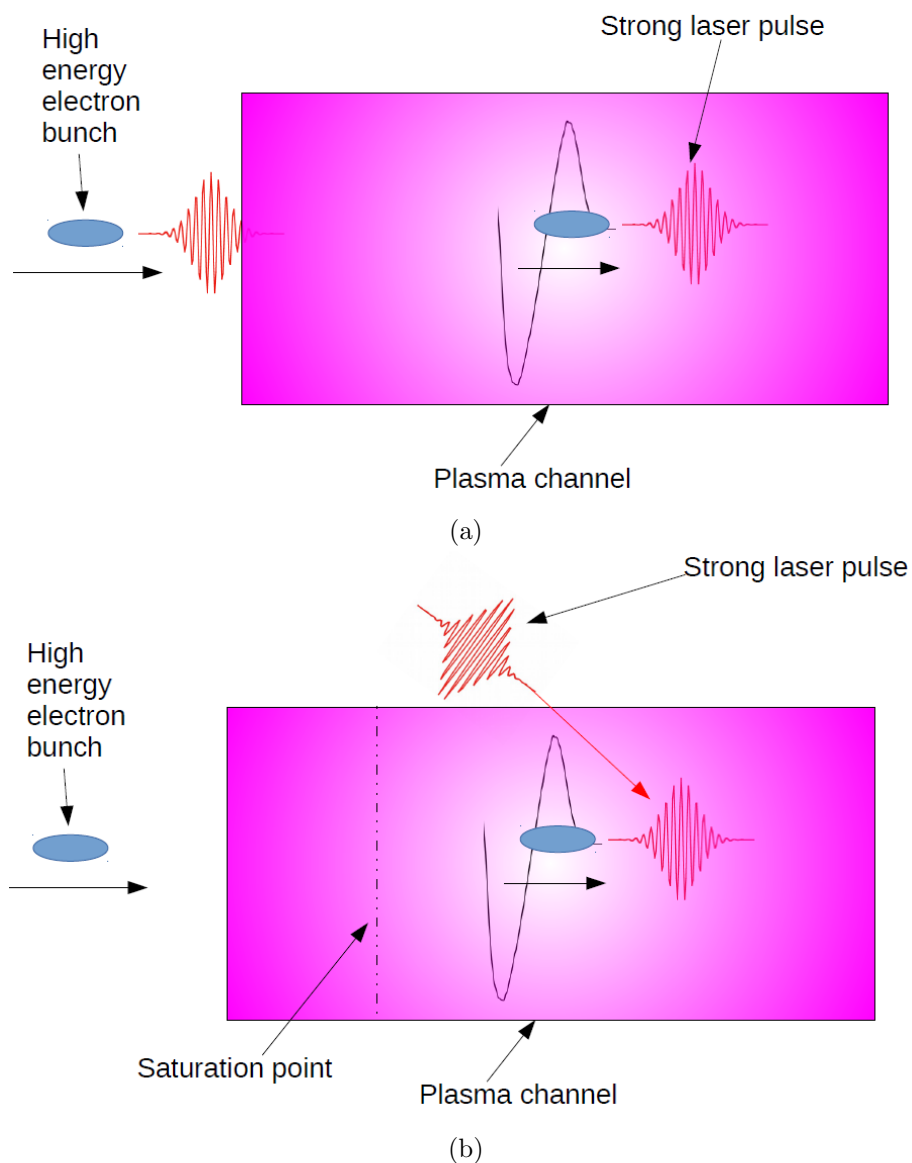


Figure 11: Schematic diagrams of active beam dumps where (a) the laser pulse is injected simultaneous to the beam and where (b) the laser pulse is injected into a passive beam dump at some later point where the beam has reached saturation for a second time. In both cases, the beam sits in the decelerating region of the wakefield created by the strong laser pulse such that the head electrons also lose energy.

Another issue that may require further investigation is the self-injection of plasma electrons in to the wakefields, particularly in the highly non-linear regime where the generated wakefield is very strong. Whereas this is considered a potentially useful method of injecting electrons in to plasma accelerators, this effect could potentially be a huge drawback of plasma beam dumps, as the electrons captured from the plasma may be re accelerated and therefore harmful. I. Kostyukov et al. [17] gives an analytical model for this self-injection for both laser and particle driven wakefields. In terms of how to measure this effect in simulations, the current in the longitudinal direction due to the plasma electrons would need to be analysed at regular intervals as the beam travels. This could also be compared for different plasma densities to investigate the linear and non-linear wakefield regimes.

An even more advanced idea, mentioned briefly by M. Kando et al. [18] is to recover the energy dumped into the plasma. T.Tajima & A.Chao originally applied for a patent for such an energy recovery beam dump in 2008, in which the plasma oscillations could be used to induce a current in a metal loop within the plasma. In this scheme, the energy from the beam is instead converted into useful electricity rather than wasted as heat in the plasma.

6 Conclusion

In conclusion this project has successfully demonstrated that plasmas can indeed potentially provide a compact solution to the problem of dumping the energy of an accelerated particle beam, with the energy of a 1 GeV beam being reduced to below 10% of it's original value over lengths of around 10 cm. The issue of energy loss saturation has been addressed in this project where it was found that using a linearly increasing plasma density provided the most efficient removal of re accelerated beam electrons. In addition, this project provides many opportunities for further work, for example the use of laser pulses to create an active beam dump that could fully decelerate the beam electrons.

Acknowledgements

Many thanks to Keiran Hanahoe, Yangmei Li and Yuan Zhao for help with setting up and using the EPOCH code.

References

- [1] W. P. Swanson, "Activation of Aluminum Beam Dumps by High-Energy Electrons at SLAC," *Health Phys.*, vol. 28, no. SLAC-PUB-1406, pp. 495–502, 1974.
- [2] R. Appleby, L. Keller, T. W. Markiewicz, A. Seryi, D. Walz, and R. Sugahara, "The International Linear Collider beam dumps," in *Proceedings, 2005 International Linear Collider Physics and Detector Workshop and 2nd ILC Accelerator Workshop (Snowmass 2005)*, 2006.
- [3] E. Esarey, P. Sprangle, J. Krall, and A. Ting, "Overview of plasma-based accelerator concepts," *Plasma Science, IEEE Transactions on*, vol. 24, pp. 252–288, April 1996.

- [4] T. D. Arber, K. Bennett, C. S. Brady, A. Lawrence-Douglas, M. G. Ramsay, N. J. Sircombe, P. Gillies, R. G. Evans, H. Schmitz, A. R. Bell, and C. P. Ridgers, “Contemporary particle-in-cell approach to laser-plasma modelling,” *Plasma Physics and Controlled Fusion*, vol. 57, pp. 1–26, Nov. 2015.
- [5] P. A. Walker, P. Alesini, A. Alexandrova, M. P. Anania, N. Andreev, I. Andriyash, A. Aschikhin, R. Assmann, T. Audet, A. Bacci, *et al.*, “Horizon 2020 EuPRAXIA design study,” in *Journal of Physics: Conference Series*, vol. 874, p. 012029, IOP Publishing, 2017.
- [6] H. Bethe, “Zur theorie des durchgangs schneller korpuskularstrahlen durch materie,” *Annalen der Physik*, vol. 397, no. 3, pp. 325–400.
- [7] F. Bloch, “Zur bremsung rasch bewegter teilchen beim durchgang durch materie,” *Annalen der Physik*, vol. 408, no. 3, pp. 285–320.
- [8] H.-C. Wu, T. Tajima, D. Habs, A. Chao, and J. Meyer-ter Vehn, “Collective deceleration: toward a compact beam dump,” *Physical Review Special Topics-Accelerators and Beams*, vol. 13, no. 10, p. 101303, 2010.
- [9] S. Ichimaru, *Basic principles of plasma physics : a statistical approach*. Frontiers in physics, Reading, Mass: Addison-Wesley, 1973.
- [10] A. Dinklage, *Plasma Physics Confinement, Transport and Collective Effects*. Lecture Notes in Physics, 670, 2005.
- [11] G. A. Mourou, T. Tajima, and S. V. Bulanov, “Optics in the relativistic regime,” *Rev. Mod. Phys.*, vol. 78, pp. 309–371, Apr 2006.
- [12] W. Lu, C. Huang, M. M. Zhou, W. B. Mori, and T. Katsouleas, “Limits of linear plasma wakefield theory for electron or positron beams,” *Physics of Plasmas*, vol. 12, no. 6, p. 063101, 2005.
- [13] K. Hanahoe, G. Xia, M. Islam, Y. Li, Ö. Mete-Apsimon, B. Hidding, and J. Smith, “Simulation study of a passive plasma beam dump using varying plasma density,” *Physics of Plasmas*, vol. 24, no. 2, p. 023120, 2017.
- [14] K. S. Kunz and R. J. Luebbers, *The finite difference time domain method for electromagnetics*. CRC press, 1993.
- [15] J. D. Hunter, “Matplotlib: A 2D graphics environment,” *Computing In Science & Engineering*, vol. 9, no. 3, pp. 90–95, 2007.
- [16] A. Bonatto, C. Schroeder, J.-L. Vay, C. Geddes, C. Benedetti, E. Esarey, and W. Leemans, “Passive and active plasma deceleration for the compact disposal of electron beams,” *Physics of Plasmas*, vol. 22, no. 8, p. 083106, 2015.
- [17] I. Kostyukov, E. Nerush, A. Pukhov, and V. Seredov, “Electron self-injection in multidimensional relativistic-plasma wake fields,” *Phys. Rev. Lett.*, vol. 103, p. 175003, Oct 2009.
- [18] M. Kando, H. Kiriya, J. Koga, S. Bulanov, A. Chao, T. Esirkepov, R. Hajima, and T. Tajima, “Opportunities for TeV Laser Acceleration,” in *AIP Conference Proceedings*, vol. 1024, pp. 197–207, AIP, 2008.

Appendix: Risk Assessment

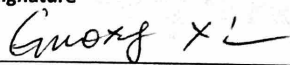
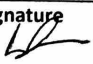
MPhys Project Risk Assessment

Title of project/experiment/activity A Compact Plasma Beam Dump for Next-Generation Particle Accelerators			
Location of activity Schuster Building – Annexe, Mezzanine and 3 rd floor computer cluster.		Start and end dates 30/01/18 to 11/05/18	
Brief description (or attach procedure/protocol) This project will involve investigating different plasma beam dump schemes . This is in order try and address the concern with conventional beam dumps, mainly the cost, size and radiological safety of them. This will done by carrying out simulations using EEPOCH software, with the analysis of data being done using Python and Visit.. As the project will almost completely consist of computer simulations and data analysis, the work will be carried out on personal laptops and computers in the Schuster Building.			
Hazard	Who is at risk?	Risk Evaluation	Control measures
Display screen equipment	Students	Adequately controlled using current safety precautions.	If using a screen for more than 10 hours a week (which we are), make sure regular breaks are taken.
Portable electrical equipment	Students	Adequately controlled using current safety precautions.	Do not consume food or drink near portable electrical equipment as this could increase the risk of electrical shocks. Ensure all equipment has undergone recent electrical safety tests.
Obstructions likely to cause tripping/falling	Students/members of staff	Adequately controlled using current safety precautions.	Ensure all wires and bags are safely stowed underneath desks to minimise any risk of trips and falls.
Personal Protective Equipment required [eye/face protection, respiratory protection, gloves, lab coat etc] N/A			
Emergency Instructions & First Aid Follow Guidelines set out in the “Out of Hours Safety Induction for the Schuster Building” PowerPoint presentation – this gives instructions of what to do if faced with an emergency.			
Any special monitoring required [e.g. hearing test, vibration monitoring, health surveillance]			

MPhys Project Risk Assessment

N/A
Further control measures required? If yes, list with actions.
N/A
Biological/Laser/Radiation Approval <i>[requires relevant Specialist Safety Officer signature and date]</i>
N/A
Out of hours/Lone working
Follow Out of Hours Guidelines: Read the relevant risk assessment and safety induction PowerPoint. Answer the questions in the health and safety assessment and obtain 100%. Tick a box to acknowledge that you have read the out of hours permission form and will abide by the rules.

Signature to confirm that this is a suitable and sufficient assessment of risk and that stated control measures are in place. This risk assessment should be reviewed if additional risks not covered in this assessment are identified or if there is any reason to indicate that the control measures are insufficient.

Name of Supervisor Guoxing Xia	Signature 	Date 10/05/2018
Name of Student 1 Thomas Bullingham	Signature T. Bullingham	Date 1/5/2018
Name of Student 2 Lewis Boulton	Signature 	Date 04/05/2018